Current Genetics (2023) 69:235–249
https://doi.org/10.1007/s00294-023-01273-3

ORIGINAL ARTICLE

TOF1 and *RRM3* reveal a link between gene silencing and the pausing of replication forks

Kholoud Shaban[1] · Andrew Dolson[1] · Ashley Fisher[1] · Emma Lessard[1] · Safia Mahabub Sauty[1] · Krassimir Yankulov[1]

Received: 16 February 2023 / Revised: 1 June 2023 / Accepted: 14 June 2023 / Published online: 22 June 2023

Abstract

Eukaryotic DNA replication is accompanied by the disassembly and reassembly of nucleosomes and the transmission of epigenetic marks to the newly assembled chromatids. Several histone chaperones, including CAF-1 and Asf1p, are central to these processes. On the other hand, replication forks pause at numerous positions throughout the genome, but it is not known if and how this pausing affects the reassembly and maintenance of chromatin structures. Here, we applied drug-free gene silencing assays to analyze the genetic interactions between *CAC1*, *ASF1*, and two genes that regulate the stability of the paused replisome (*TOF1*) and the resumption of elongation (*RRM3*). Our results show that *TOF1* and *RRM3* differentially interact with CAF-1 and *ASF1* and that the deletions of *TOF1* and *RRM3* lead to reduced silencing and increased frequency of epigenetic conversions at three loci in the genome of *S. cerevisiae*. Our study adds details to the known activities of CAF-1 and Asf1p and suggests that the pausing of the replication fork can lead to epigenetic instability.

Keywords Replication fork pausing · *TOF1* · *RRM3* · CAF-1 · *ASF1* · Epigenetic conversions

Introduction

Gene silencing in *S. cerevisiae* has served as a paradigm for complex chromatin-mediated phenomena in other eukaryotes. In this organism, the silencing of genes at the mating type loci *HMRa* and *HMLα*, the sub-telomeric regions of the chromosomes, and the rRNA-encoding DNA (the *rDNA*) have received significant attention (Sauty et al. 2021; Shaban et al. 2021). At these positions, the Histone Deacetylase (HDAC) Sir2p and the associated Silent Information Regulator (Sir) proteins initiate and maintain a cascade of spreading of histone deacetylation along the adjacent nucleosomes (Rusche et al. 2003). This activity leads to a meta-stable alternating between active and silent states of reporter genes inserted in the sub-telomeres or *rRNA* gene loci (Rusche et al. 2003). The mating type loci are robustly repressed and constitutively silent but can show alternating active/silent states upon compromised silencing (Rusche et al. 2003; Yankulov 2013). A similar meta-stable phenotype is observed at the *FLO* genes loci; however, the silencing at these positions is independent of the *SIR* genes (Sauty et al. 2021; Shaban et al. 2021).

The mechanisms of *SIR*-mediated gene silencing are well characterized (Gartenberg and Smith 2016). In comparison, the mechanisms of maintenance of the epigenetic state through multiple rounds of cell divisions and passages of the replication forks are insufficiently addressed (Rowlands et al. 2017). The current models for histone turnover during DNA replication and the preservation of epigenetic state have been recently summarized in (Stewart-Morgan et al. 2020; Shaban et al. 2021). Briefly, as the replication fork advances, the nucleosomes are disassembled and the "old" histones are ferried behind the fork through the activity of the Asf1p and FACT histone chaperones. Behind the fork another histone chaperone, the Chromatin Assembly Factor 1 (CAF-1), is assembling H3/H4 tetramers. Recently, it has been shown that the MCM helicase, and the Dbp3–Dbp4 subunits of DNA polymerase ε and Ctf4p are involved in the symmetric distribution of H3/H4 tetramers (Gan et al. 2018; Petryk et al. 2018; Yu et al. 2018), thus leading to the suggestion that the CAF-1 function is restricted to filling-in the gaps by assembling H3/H4 from "new" dimers delivered from the cytoplasm (Ahmad and Henikoff 2018; Groth et al.

Communicated by M. Polymenis.

✉ Krassimir Yankulov
yankulov@uoguelph.ca

[1] Department of Molecular and Cellular Biology, University of Guelph, Guelph, ON N1G2W1, Canada

2007; Almouzni and Cedar 2016). However, earlier studies have suggested that CAF-1 could have additional functions at certain loci where the "old" H3/H4 tetramers can be lost (Almouzni and Cedar 2016; Rowlands et al. 2017). After the reassembly of nucleosomes behind the fork, the epigenetic marks on the old histones are copied onto the new ones by a largely unknown mechanism (Ahmad and Henikoff 2018).

It is known that replication forks slow down and/or pause at numerous positions occupied by proteins that are tightly bound to DNA or at active gene promoters (Ivessa et al. 2003; Makovets et al. 2004; Azvolinsky et al. 2006; Shyian and Shore 2021). Frequent fork pausing has been detected in the *rRNA* gene loci and in the sub-telomeres, especially in the absence of Rrm3p, a DNA helicase necessary for the release of the paused forks in vivo but not for efficient fork progression in experiments conducted with purified/recombinant proteins in vitro (Azvolinsky et al. 2006; Deegan et al. 2019). Analyses of fork stalling at natural or engineered protein barriers have revealed that mammalian homologues of *RRM3* (RTEL1, DDX11, FANCJ, and DHX36) and other helicases or scaffold proteins (BLM and FANCM) operate to restart/repair the stalled replisomes (Shyian and Shore 2021; Scully et al. 2021). Forks also stall at sites of DNA damage and possibly at sites of stable secondary DNA structures (Shyian and Shore 2021). However, the role of *RRM3* and its homologues under these conditions is not clear.

The Fork Protection Complex (FPC, built-up of Mrc1p/Csm3p/Tof1p) is known to stabilize the paused forks and ensure the timely resumption of elongation. The FPC is also crucial for processive elongation in vitro (Yeeles et al. 2017). Additional functions of Tof1p include the recruiting of FACT to the fork (Safaric et al. 2022) and linking FPC to the function of Topoisomerase I (*TOP1*). More specifically, the C-terminus of Tof1p is required for the recruitment of Top1p to proteinaceous fork barriers, but not for the activation of DNA replication checkpoints (Shyian et al. 2020). Prior genetic studies have demonstrated that the effects of *TOF1* deletion at the *rRNA* gene arrays are counteracted by deletion of *RRM3* (Mohanty et al. 2006; Bastia et al. 2016). However, a recent study added that the functions of *RRM3* and *TOF1* can be separated in vivo, suggesting that these factors act independently of each other (Shyian et al. 2020). How the activities of *RRM3* and *TOF1* and fork pausing affect histone turnover and the maintenance of chromatin state remains unclear.

We have recently shown that the deletion of *RRM3* exacerbated the silencing defects observed at the telomeres and at the *FLO11* loci upon the deletion of *CAC1* (the gene that encodes the largest subunit of CAF-1) (Wyse et al. 2016; Rowlands et al. 2017). In this study, we asked how *TOF1* and *RRM3* genetically interact with the H3/H4 histone chaperones involved in the replication-coupled reassembly of nucleosomes.

Materials and methods

Yeast strains

Strains with single gene deletions were obtained from Open Biosystems or were gifts from other labs (see S1 Table). Double deletion mutants of *tof1* with *cac1, rrm3,* and *asf1* were generated by direct knockout of *TOF1* with PCR fragments or by routine mating/sporulation lab techniques. *The tof1-726*Δ and the *tof1-830*Δ derivatives were produced by PCR-mediated knockout of ASF1, CAC1, and RRM3 in the strains provided by (Westhorpe et al. 2020). All gene deletions were confirmed by PCR prior and after each genetic manipulation. *JRY0803* and its derivatives were used in the CRASH assay as in (Janke et al. 2018). All strains were routinely maintained at 30 °C on Yeast Extract Peptone Dextrose YPD (1% yeast extract, 2% tryptone, and 2% glucose) media. Flow cytometry and fluorescent microscopy experiments were conducted with cells grown in Synthetic Complete (SC) media and SC drop-out media, as required.

Growth rates' analysis

Strains were serially diluted in a 96-well plate and the OD_{600} of the exponentially growing cultures was measured every 2 h for a period of 24 h using infinite 200Pro plate reader with continuous shaking. The data were analyzed in the MS Excel®.

Methyl methane sulfonate (MMS) sensitivity

Cells from exponentially growing cultures were serially diluted in a 96-well tray plate and 5 µl aliquots were spotted on plates with different MMS concentrations [0.05%, 0.1% and 0.2% MMS (Sigma)]. Plates were incubated at 30 °C for 2 days and images were taken by regular photography.

Cell cycle analysis

Cells in early exponential phase were arrested by 15 µg/mL Nocodazole for three hours at 30 °C. Cells were washed twice and resuspended in YPD medium, and samples were collected at different time points after the release from the block. Cells were then fixed with 70% Ethanol and DNA was stained with Propidium Iodide as in (Jeffery et al. 2015). Cell cycle analysis was done using Sony SH800z flow cytometer and *LESH-00SZFCPL*™ software**.**

HTB1-yEGFP-URA3-tel, FLO11-yEGFP, and CRASH reporters

An *yEGFP* reporter driven by the Histone H2B promoter (HTB1) (*HTB1-yEGFP)* from pFOM298 plasmid

(Mano et al. 2013) was cloned into the *pUCAIV* plasmid (Gottschling et al. 1990) to produce the *ADH4-HTB1-yEGFP-URA3-tel* construct for insertion into the *VIIL* telomere. The *HTB1-yEGFP* reporter was inserted in both orientations relative to the telomere (Fig S1.A). It was found that the reverse orientation toward telomere produced higher proportions of GFP + cells and signals and all subsequent experiments were conducted with this construct. The *FLO11-yEGFP* reporter was produced by replacing the *FLO11 ORF* at its genome location with *yEGFP-KanMX* construct as described in (Rowlands et al. 2019b) (Fig S1.B). The strains for CRASH analyses contain an expression cassette for the *CRE* recombinase inserted in the *HML* locus as described in (Janke et al. 2018) (Fig S1.C). Genome manipulation in all strains was confirmed by PCR.

Analysis of yEGFP signals by fluorescent microscopy

Cell suspensions were grown to saturation in SC media. After vigorous vortexing to disperse cell clusters, images were acquired by non-confocal Leica DM 6000B microscope with bright field and fluorescent field at 40X and 100X immersion oil lenses. Alternatively, cells' cultures were serially diluted in a 96-well plate and incubated at 25 °C overnight, and images were acquired by Diskovery™ Spinning Disk confocal microscope with 60X lens. All images were processed and analyzed by *Volocity*™ software as in (Rowlands et al. 2019b). Briefly, the pixel values of at least 25 ROIs (Region of Interest) with no cells were used to calculate the average background for each individual experiment. Next, pixel values in at least 25 ROI over whole single isolated cells with no visible signal in them were acquired and used as a postulated arbitrary threshold line. Finally, pixel values of ROI over all cells in three separate fields with 50–100 cells were measured. Distribution graphs of the raw intensity signals are shown in Supplemental Materials (Fig. S4).

The accuracy of the postulated threshold lines between experiments was evaluated by the prediction approaches of the statistical decision theory (Hastie et al. 2009). This algorithm showed that a threshold level of 160% of the average background identifies positive cells with 100% accuracy (Fig S2, S3). For negative cells, accuracy was greater than 90% (Fig S2, S3). We used this threshold in each individual experiment with all strains tested. At least three separate experiments were conducted with each strain. Average numbers and standard deviations were calculated in Excel®.

CRASH (cre-reported altered states of heterochromatin) assays

The CRASH assay was performed as described previously (Janke et al. 2018; Rowlands et al. 2019b). The strains for this assay contain an *RFP/yEGFP* switch reporter cassette that converts the expression of RFP to yEGFP upon the expression of *CRE* (Fig. S1.C). Briefly, cells were grown on the appropriate SC drop-out plates containing 300 µg/mL hygromycin to select for the initial 100% RFP positive state. A single colony from this plate was dispersed in SC medium and cells were plated on appropriate drop-out media based on their knockout markers at 50–100 colonies per plate. Colonies were imaged after 5–7 days growth using a Zeiss AxioZoom V16 microscope at 2X magnification equipped with a Hamamatsu Camera and Zen software. The de-repression events for each single and double mutant could be visualized by green segments that could be counted. Counting of green segments was done for 4–5 individual colonies from each strain except for some double mutants where the multiplicity of green segments precludes accurate counts. Statistical analyses were performed, and graphs were built using the MS Excel®.

Flow cytometry

Cells were grown until they reached an exponentially growing state of $OD_{600} = 1.0$, and cells were harvested and followed by sonication to be dispersed. They were suspended in Phosphate-Buffered Saline (PBS) prior to analysis by a Sony SH800z flow cytometer. The *LESH00SZFCPL*™ software was used to collect data. Isogenic strains with no yEGFP reporters were used to set up the gates for GFP-negative cells. Three independent experiments were conducted with each strain. Graphs were produced and analyzed by the MS Excel®.

Measurement of conversions rates

Strains were grown in SC medium and briefly sonicated to disperse cell aggregates. The cultures were then diluted to about 3–5 cell/ml and 200 µl aliquots were dispensed in three 96-well plates. The plates were incubated at 25 °C until a single cluster of cells could be seen at low magnification of the microscope. Under these conditions, most of these mini-cultures originate from a single cell and go through about 8–11 generations. Cells from single clusters were then dispersed and analyzed by flow cytometry to determine the percentage of GFP + cells in each colony. Data analysis and Graphs were made in the MS Excel®.

Results

Experimental strategy

It has been previously shown that the loss of gene silencing at the sub-telomeric and *FLO11* loci in *cac1*Δ and *asf1*Δ

strains is exacerbated by the deletion of *RRM3* (Wyse et al. 2016; Rowlands et al. 2019b) and that the deletions of *RRM3* or *TOF1* have opposite effects on the pausing of replication forks at the *rRNA* gene array (Mohanty et al. 2006). It remains unclear if and how *TOF1* is contributing to gene silencing. To address this question, we produced a series of double deletion mutants of *CAC1, ASF1* along with *RRM3* and *TOF1*. We attempted the production of *cac1*Δ*mrc1*Δ and *asf1*Δ*mrc1*Δ mutants, but these strains were not viable. In the viable strains, we inserted *yEGFP* reporters in two loci that display gene silencing and on/off "variegated" patterns of gene expression. At the *FLO11* locus, the reporter is driven by the *FLO11* promoter itself (Rowlands et al. 2019b). In the *VIIL* telomere, we inserted the *URA3-HTB1-yEGFP1* construct in which *yEGFP* is driven by the strong Histone H2B promoter (HTB1) (Mano et al. 2013; Shaban et al. 2023). This construct faithfully recaptures most of the effects observed previously by *URA3* reporters and precludes the use of the toxic 5-FOA (Mano et al. 2013; Shaban et al. 2023). It also provides strong yEGFP signals that can be evaluated by drug-free flow cytometry and/or fluorescent microscopy assays. Previous reports had indicated that the repression of the native *HTB1* gene was dependent on the activity of *ASF1* and other histone chaperones and the adjacent *Yta7* chromatin boundary (Sutton et al. 2001; Zunder and Rine 2012). However, the *HTB1-yEGFP* construct does not contain the boundary and in our hands does not demonstrate sensitivity to the deletion of *ASF1*, while the deletion of *ASF1* reduced silencing at the *FLO11* and *HML* loci (see below).

At the mating *HMLα* locus, we measured the levels of silencing by a *CRE* expression cassette and the CRASH assay (Janke et al. 2018; Brothers and Rine 2019).

At the *VIIL* and *HMLα* loci, gene silencing is critically dependent on the recruitment and activity of Sir2p HDAC, while *FLO11* silencing is independent of the *SIR* genes.

Characteristics of the double deletion mutants.

First, we checked some general characteristics of the produced strains. Growth rates were measured in liquid cultures in 96-well trays on a shaking platform supplied with a spectrophotometer. In agreement with the previous studies, the *cac1*Δ, *rrm3*Δ, *tof1*Δ, and *asf1*Δ strains showed little loss in growth rates as compared to the isogenic *BY4742* strain (Park and Sternglanz 1999; Jeffery et al. 2013; Wyse et al. 2016) (Fig. 1A). The double mutants *tof1Δcac1Δ* and *tof1Δrrm3Δ* also did not show any major growth defects. However, a decrease in growth rate was detected in the *tof1Δasf1Δ* double mutant (Fig. 1A). Analyses of cell cycle progression after arrest with Nocodazole revealed that the reduced growth rate of *tof1Δasf1Δ* cultures should be attributed to a very slow progression through G1/S phases (Fig. 1B). The *tof1*Δ cells showed minor cell cycle defects as compared to *BY4742*. Interestingly, *asf1*Δ cells were slow in exiting mitosis. At present, we have no good explanation for this effect of *asf1*Δ.

All strains were also tested for sensitivity to DNA damage by exposure to 0.05%, 0.1%, and 0.2% MMS (Fig. 1C). MMS methylates guanine and adenine bases leading to mispairing, replication blocks, point mutations, and double-stranded DNA breaks (Beranek et al. 1983). We used a *mrc1*Δ strain as a control. Consistent with the previous studies, the deletions of *CAC1, RRM3,* and *ASF1* marginally increased sensitivity to this mutagen (Tyler et al. 1999; Jeffery et al. 2013; Wyse et al. 2016). The deletions of *TOF1* and *MRC1* had a stronger effect relative to the *cac1*Δ, *asf1*Δ, and *rrm3*Δ strains. The double deletions *tof1Δcac1Δ* and *tof1Δrrm3Δ* did not display higher sensitivity as compared to the single mutants. However, the deletion of both *TOF1* and *ASF1* lead to an additive sensitivity to this type of DNA damage, thus reiterating a possible *ASF1-TOF1* functional link. Similar increased sensitivity to DNA damage has been earlier observed in *cac1Δrrm3Δ* (Rowlands et al. 2019b).

We also noticed that the *tof1Δasf1Δ* strain formed small clusters of cells in liquid cultures (Fig. 2D). The clusters were smaller than the ones previously observed in *cac1Δasf1Δ, rrm3Δasf1Δ,* and *cac1Δrrm3Δ* strains (Rowlands et al. 2019b). This mild flocculation phenotype was only moderately enhanced in the presence of Nicotinamide (not shown). None of the other strains displayed flocculation.

Analysis of HTB1-yEGFP expression at the VIIL telomere

Previous studies have pointed out that the deletion of *CAC1* and, to less extent, the deletion of *ASF1* and *RRM3* lead to loss of silencing at the *VIIL* telomere as measured by a *URA3* reporter and sensitivity to 5-FOA (Zhang et al. 2000; Jeffery et al. 2013; Wyse et al. 2016). We revisited these phenotypes by Flow Cytometry and fluorescent microscopy assays with the *URA3-HTB1-yEGFP-tel* construct (Fig. 2). We also tested the effects of deletion of *TOF1* in *BY4742*, *cac1*Δ, *asf1*Δ, and *rrm3*Δ genetic backgrounds. In these assays, the increase of the percentage of GFP-positive cells indicates loss of silencing and the decrease indicates reversal of the loss.

In agreement with the previous studies, in both flow cytometry and microscopy experiments, the deletion of *CAC1* was accompanied by an increase in the percentage of yEGFP$^+$ cells (Fig. 2A, B). The deletion of *ASF1* did not show statistically significant changes in the expression of the *HTB1-yEGFP* construct as compared to *BY4742* (Fig. 2A, B). Surprisingly, and in disagreement with prior experiments with the *URA3*/5-FOA assays, in the *rrm3*Δ strain, the flow cytometry analyses indicated a statistically significant

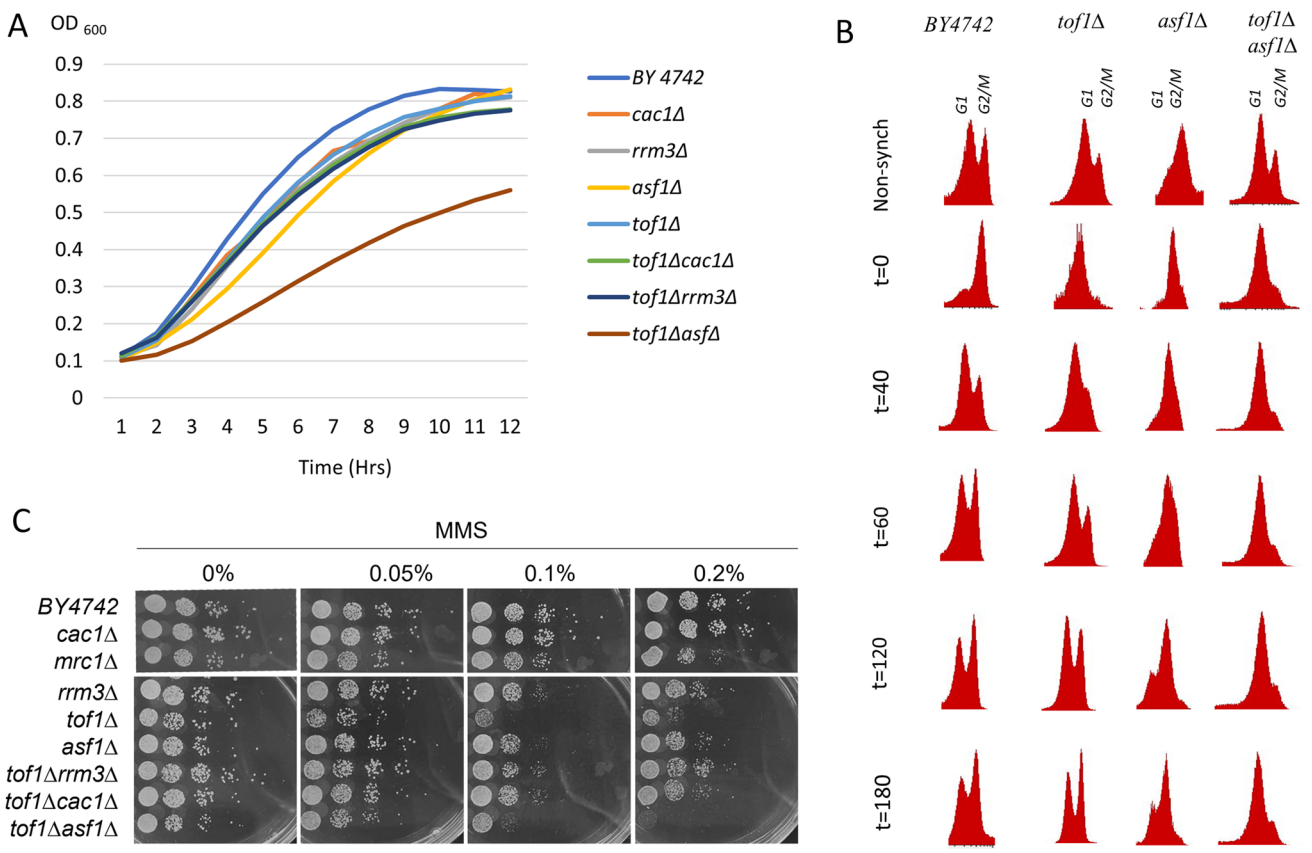

Fig. 1 Characteristics of the mutant strains. (**A**) Growth rates analysis. Cells from exponentially growing cultures were diluted in a 96-well plate and the OD_{600} was measured every 2 h for a period of 24 h. The graphs were made using the MS Excel®. (**B**) Cell Cycle analysis. Exponentially growing cells were arrested by Nocodazole and then released from the arrest, and samples were collected at the indicated time points and stained with Propidium Iodine. (**C**) MMS sensitivity. Cells from an exponentially growing cultures were serially diluted and aliquots were spotted on plates with different concentrations of MMS (0.005%, 0.01%, and 0.02%). One of two independent experiments is shown

decrease in the proportion of yEGFP$^+$ cells (Fig. 2A), while fluorescent microscopy detected no difference between the *BY4742* and *rrm3*Δ cells (Fig. 2B). It is possible that these discrepancies are caused by the effect of 5-FOA on the pools of dNTPs (Rossmann et al. 2011; Takahashi et al. 2011) in conjunction with the deletion of *RRM3*. The deletion of *TOF1* also decreased in the proportion of yEGFP$^+$ cells as measured by flow cytometry but not by microscopy (Fig. 2A, B). Hence, a possible anti-silencing effect of the individual deletions of *RRM3* or *TOF1* at the *VIIL* telomere seems subtle and is not conclusively established by our yEGFP-based assays.

Next, we tested the silencing of the *HTB1-yEGFP* reporter in the double deletion mutants. The deletion of *TOF1* in the *cac1*Δ strain increased silencing as demonstrated by the reduction in the proportion of yEGFP$^+$ cells (Fig. 2A, B). Conversely, in the *asf1*Δ background the deletion of *TOF1* increased the proportion of yEGFP + cells suggesting a decreased silencing of the *HTB1-yEGFP* reporter (Fig. 2A, B). These results demonstrate that the *TOF1* and *RRM3* genes, similar to their effect on paused replication forks (Mohanty et al. 2006), have opposite functions in the silencing at the *VIIL* telomere. In the *rrm3*Δ background, the deletion of *TOF1* increased the proportion of yEGFP$^+$ as measured by flow cytometry, but this result was not confirmed by the microscopy experiments.

In agreement with our prior studies, we observed a substantial loss of gene silencing at the *VIIL* telomere in the *cac1Δrrm3*Δ, *asf1Δcac*Δ, and *asf1Δrrm3*Δ mutants by both flow cytometry and fluorescent microscopy (Fig. 2A, B), but not to the extent detected by the *URA3*/5-FOA assay (Jeffery et al. 2013; Wyse et al. 2016; Rowlands et al. 2019b).

Earlier structure–function analyses of *TOF1* had demonstrated that the deletion of its C-terminus beyond amino acid 762 (*tof1-762*Δ*)* precluded its interaction with Csm3p, the pausing of the fork, and the TOF-mediated sensitivity to DNA damage (Westhorpe et al. 2020). The truncation of the protein at position 830 (*tof1-830*Δ) displayed significantly milder phenotypes and did not preclude fork pausing (Westhorpe et al. 2020).

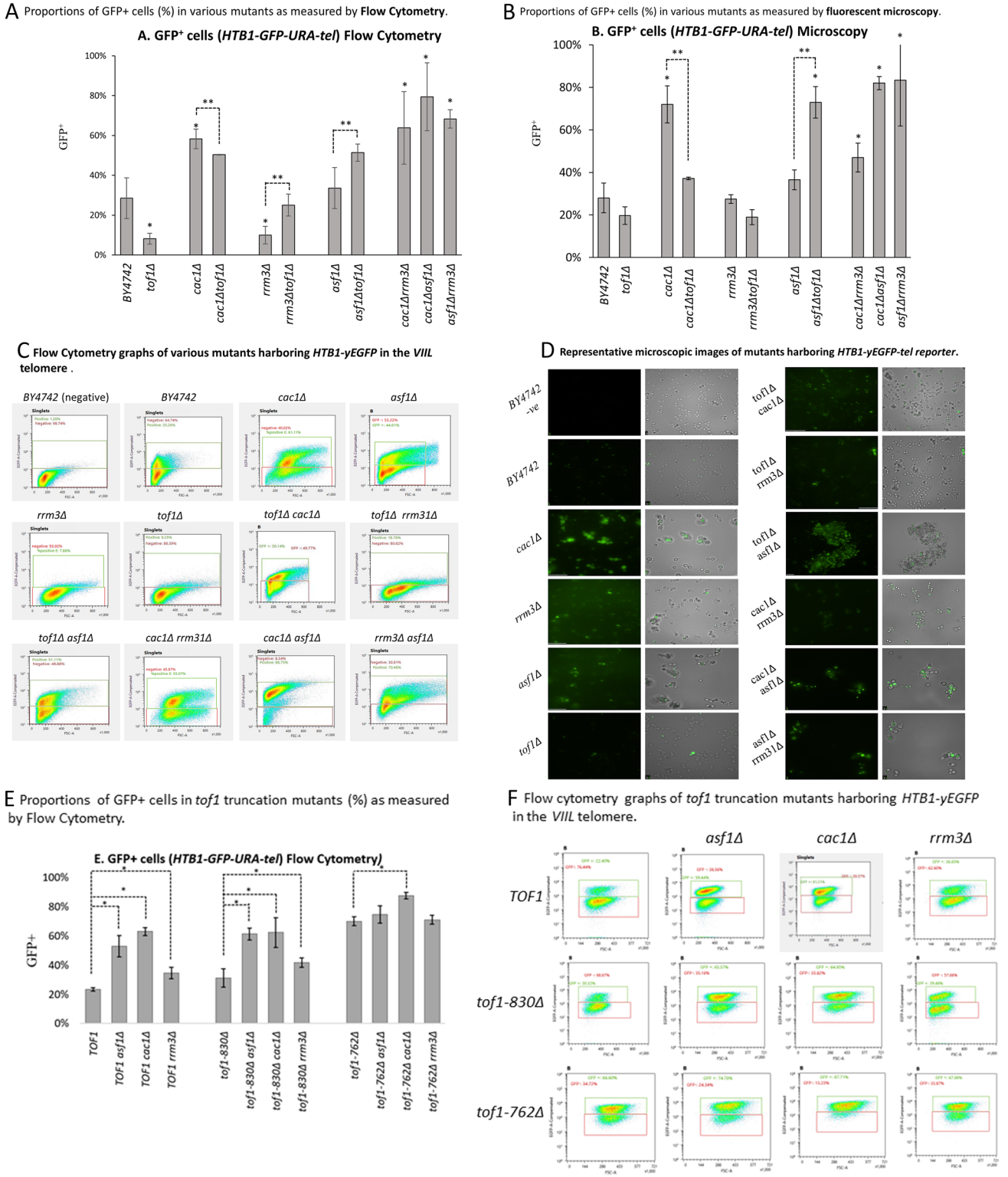

To get further insights in the mechanism of *TOF1*-mediated maintenance of gene silencing, we tested if these *tof1* mutants alter the expression of HTB1-yEGFP (Fig. 2E). The truncation at position 830 (*tof1-830Δ)* did not significantly change the expression of HTB1-yEGFP (Fig. 2E). In this genetic background, the deletions of *CAC1* and *ASF1* reduced silencing as demonstrated by the higher proportions of GFP + cells, while the deletion of *RRM3* did not have a statistically significant effect (Fig. 2E). However, the truncation at position 762 (*tof1-762Δ)* markedly reduced

◂**Fig. 2** Analyses of the expression of *HTB1-yEGFP* at the *VIIL* telomere. (**A**) Proportions of GFP^+ cells (%) in various mutants as measured by flow cytometry. (**B**) Proportions of GFP^+ cells (%) in various mutants as measured by fluorescent microscopy. Distribution graphs of the raw intensity signals are shown in Fig. S4, A. (**C**) Flow cytometry graphs of $yEGFP^+$ cells in various mutants. Cells were analyzed by Sony SH800z flow cytometer and graphs were generated by The *LESH00SZFCPL*™ Software. Gating for GFP-negative cells was based on the identical analyses of isogenic strains without the *HTB1-yEGFP* reporter. (**D**) Representative microscopy images of various mutants. Cells were analyzed by *Leica DM* 6000B microscopy and signals were processed by the *Volocity*® software. (**E**) Proportions of GFP^+ cells (%) in *TOF1*, *tof1-762*Δ, and *tof1-762*Δ strains as measured by flow cytometry. (**F**) Flow Cytometry graphs of $yEGFP^+$ cells in *tof1* mutants. * represents statistically significant difference compared to the *BY4742* strain. ** represents statistically significant difference between the two connected stains (independent *T* tests were used)

the silencing of the construct. In this strain, the deletions of *ASF1* and *RRM3* in this strain marginally increased the proportions of GFP + cells, while the deletion of *CAC1* had a statistically significant effect (Fig. 2E). We conclude that the *tof1-762*Δ allele, which is known to reduce the pausing of replication forks (Westhorpe et al. 2020), also reduced the silencing of the *HTB1-yEGFP* construct. At the same time, the genetic interactions of the *tof1-762* allele with *ASF1*, *CAC1,* and *RRM3* did not precisely phenocopy the effects of these genes observed with the complete destruction of *TOF1* (Fig. 2A).

Analyses of gene silencing at the FLO11 locus

The analyses of gene silencing at the *FLO11* locus were performed using a *yEGFP* reporter driven by the *FLO11* promoter (*FLO11-yEGFP*). Again, the increase of the percentage of GFP-positive cells indicates loss of silencing and the decrease indicates reversal of the loss. In the flow cytometry experiments, the single mutants *cac1*Δ*, asf1*Δ*, rrm3*Δ, and *tof1*Δ revealed no statistically significant increase in the expression of *yEGFP* relative to *BY4742* cells (Fig. 3A) and modest, but statistically significant increase in the proportions of GFP + cells in the microscopy experiments (Fig. 3B). Importantly, the deletion of *TOF1* in any of the *cac1*Δ*, asf1*Δ, and *rrm3*Δ strains had no substantial effect on the silencing of *FLO11-yEGFP*. On the other hand, the combination of deletions of *CAC1, ASF1,* and *RRM3* lead to a substantial increase in the number of GFP + cells. This result is in agreement with our earlier study (Rowlands et al. 2019b) in which *FLO11*-mRNA expression was substantially increased in bulk cultures of these double deletion mutants. In the current study, we reproduce this observation at a single cell resolution using a yEGFP reporter.

These results and the very modest flocculation phenotype in *asf1*Δ*tof1*Δ cells point out that *TOF1* could not play a major role at this silenced locus.

Analysis of gene silencing the HMLα locus

The silencing at the *HMLα* locus was performed by the CRASH assay as in (Janke et al. 2018). The assay utilizes a *Cre* recombinase inserted at *HML* and a separate *RFP* → *yEGFP* reporter cassette on chromosome *V*. Transient de-repression of *HMLα* would trigger the *Cre*-mediated removal of *RFP* and the expression of *yEGFP*. This irreversible effect is visualized as green segments in red colonies (Dodson and Rine 2015; Janke et al. 2018). In these assays, the increase in the number of green segments in a red colony indicates transient loss of silencing. The appearance of totally green colonies indicates loss of silencing beyond the quantitative scope of the assay. Previous studies have demonstrated that *cac1*Δ cells do not display mating defects or de-repression of *yEGFP* reporters inserted in *HMLα* (Jeffery et al. 2013). In contrast, studies with the CRASH assay in *cac1*Δ revealed numerous green segments (Janke et al. 2018; Rowlands et al. 2019b). We applied this high sensitivity assay in the mutants generated in this study. Average numbers of green segments in 4–5 colonies of each strain were calculated and plotted (Fig. 4A). Compared to *BY4742*, the *rrm3*Δ, *asf1*Δ, and *tof1*Δ colonies showed statistically significant increase in the number of green segments, with *asf1*Δ showing the least effect (Fig. 4A, B). The segments in *cac1*Δ cells were too numerous to count indicating a more profound silencing defect.

TOF1 again showed differential effects on gene silencing depending on the genetic background. In the *cac1*Δ background, the deletion of *TOF1* led to a lower countable number of the green segments thus indicating reversal of the loss of silencing (Fig. 4A, B). In contrast, the *tof1*Δ-mediated silencing defects were exacerbated in the *asf1*Δ strain. In the *rrm3*Δ strain, the deletion of *TOF1* also increased the number of green segments, but to a lesser extent as compared to *asf1*Δ (Fig. 4A, B). The *cac1*Δ*asf1*Δ, *cac1*Δ*rrm3*Δ, and *asf1*Δ*rrm3*Δ double mutants displayed predominantly green colonies thus pointing to a profound defect in *HMLα* silencing. We conclude that both *RRM3* and *TOF1* contribute to the silencing of *HMLα*. Similarly to the situation at the *VIIL* telomere (Fig. 2), they can also reduce or increase the silencing deficiencies when combined with deletions of *CAC1* and *ASF1,* respectively.

Conversion frequencies at the VIIL telomere

Positional variegation is characterized by infrequent Silent → Active and Active → Silent (S → A and A → S) conversions of the affected loci (Yankulov 2013). In an earlier study, we have used the *URA3*/5-FOA assay to show that the loss of *CAC1* could lead to lower frequency of such epigenetic conversions (Jeffery et al. 2013). Here, we have tested the effect of our mutants on the frequency

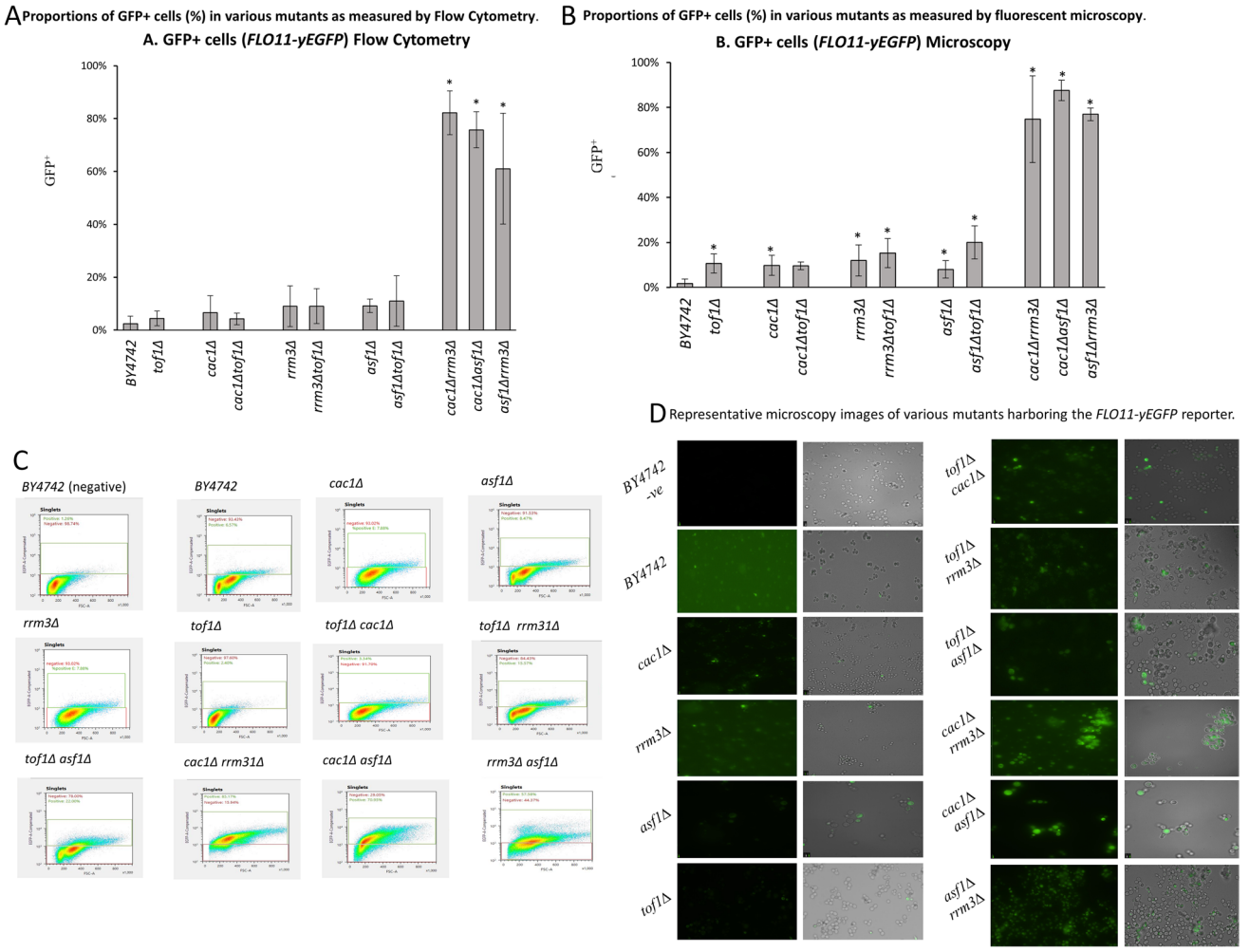

Fig. 3 Analyses of the expression of *FLO11-yEGFP*. (**A**) Proportions of GFP$^+$ cells (%) in various mutants as measured by flow cytometry. * represents statistically significant difference compared to the *BY4742* strain. ** represents statistically significant difference between the two connected stains (independent *T* tests were used). (**B**) Proportions of GFP$^+$ cells (%) in various mutants as measured by fluorescent microscopy. Distribution graphs of the raw intensity signals are shown in Fig. S4, B. (**C**) Flow Cytometry graphs of yEGFP$^+$ in various mutants. Cells were analyzed by Sony SH800z flow cytometry and graphs were generated by *LESH00SZFCPL*™ Software. Gating for GFP-negative cells was based on the identical analyses of isogenic strains without the *HTB1-yEGFP* reporter. (**D**) Representative microscopy images of various mutants. Cells were analyzed by Leica DM 6000B microscopy and signals were processed by the *Volocity*® software

of conversions of the *HTB1-yEGFP* reporter at the *VIIL* telomere. We applied a technique that was identical to the one previously used to assess the frequency of conversions of a different *yEGFP* reporter inserted at the *HMRa* locus (Jeffery et al. 2013). Briefly, cells were serially diluted in 96-well plates and grown for 8–10 generations. Mini-cultures in wells with single clusters of cells were deemed to originate from a single cell. These mini-cultures were analyzed by flow cytometry and the percentage of GFP$^+$ cells in each of them was plotted as a single bar in a plot of multiple bars (Fig. 5). The number of generations in each mini-culture was determined by the count of events in the flow cytometer and any mini-culture with less than eight or more than ten generations was excluded from further analyses. Between 30 and 50 mini-cultures were analyzed for each strain.

In parallel, we generated simulated graphs representing outcomes of the above experiment at different S → A and A → S conversion rates as in (Jeffery et al. 2013). In these simulations, we assumed that each culture originates with one single cell and a one single conversion event could take place in any of the first six generations. We also assumed that the proportions of mini-cultures in which the seeding cell will have an active or silent *HTB1-yEGFP* gene, respectively, would be similar to the proportion of GFP + cells in the bulk seeding cultures. In Fig. 5A, we present a simulation of a strain with 30% GFP + cells that has grown for 8–11 generations at 9% A → S and 5% S → A conversion rates per

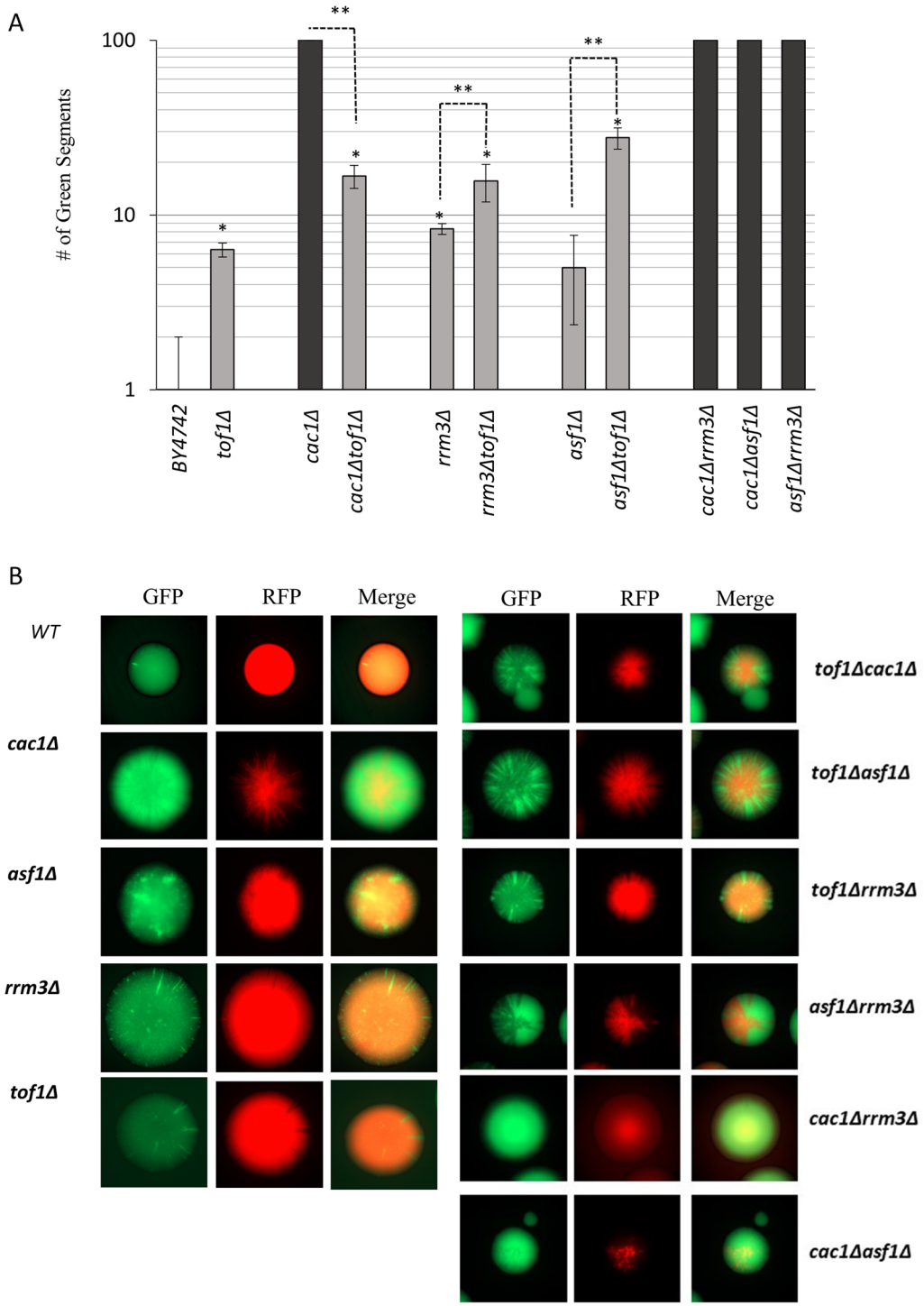

Fig. 4 Analyses of gene silencing at *HMLα* by CRASH assay. (**A**) Cells were grown in the presence of Hygromycin to select for the RFP$^+$ state of the RFP → yEGFP reporter, then streaked on SC dropout or SC/Geniticin agar, as appropriate, and grown to produce visible colonies. Images of colonies were taken with Axiozoom microscope using green and red filters and merged in Zen Software. Green sectors in 3–5 colonies were counted and plotted. ** represents statistically significant difference between the two connected stains (independent *T* tests were used). (**B**) Images of sectored colonies in various mutants

generation. In Fig. 5B, we present a simulation of a strain that has grown for 8–11 generations at 5% A → S and 3% S → A conversion rates. In these experiments, the prevalence of colonies with similar close percentage of GFP-positive cells (as represented by similar height of the multiple bars) reflect higher rate of epigenetic conversions. The appearance

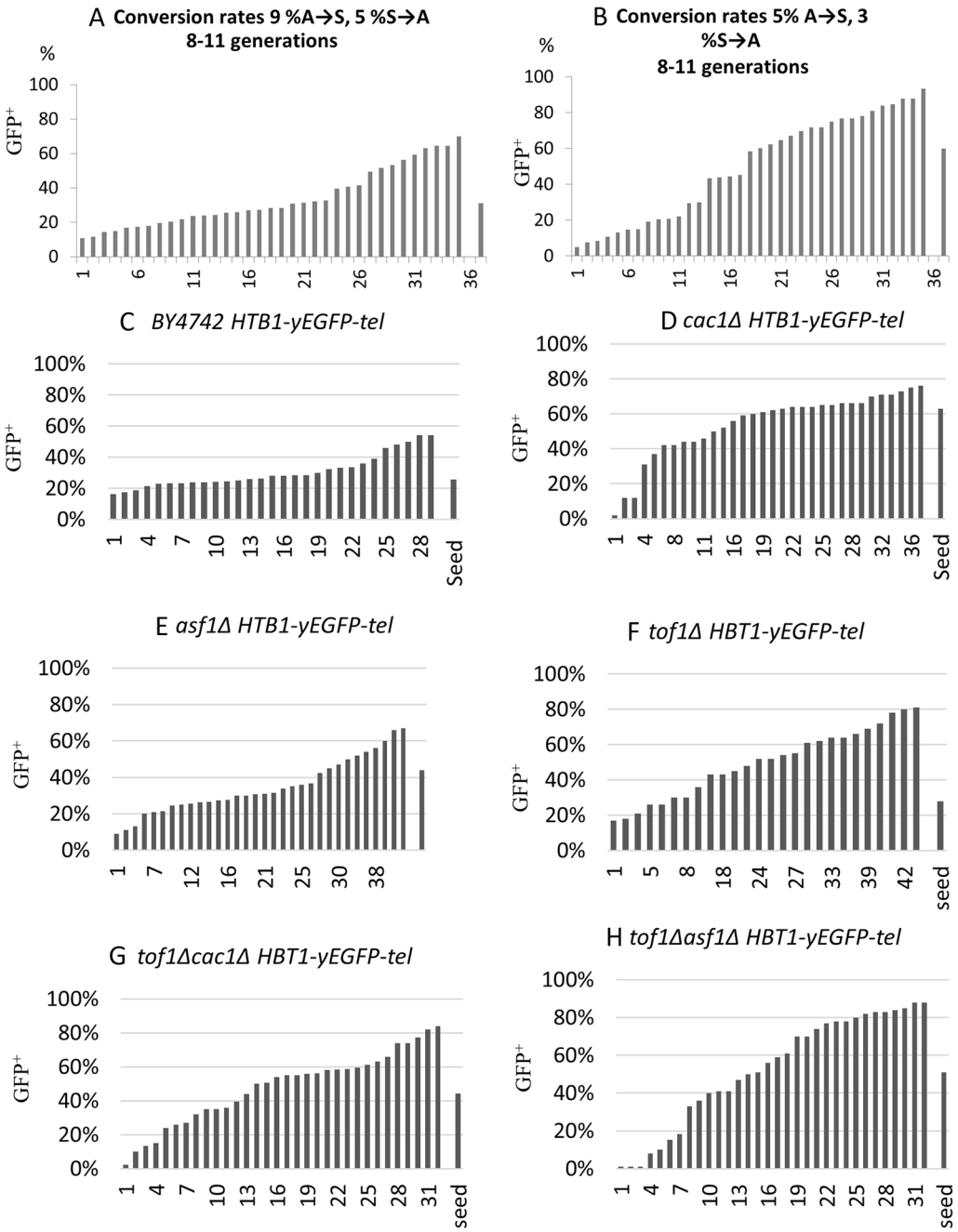

Fig. 5 Measurements of conversion rates of at the *VIIL* telomere. Mini-cultures originating from a single cell were grown for 8–10 generations and analyzed by flow cytometry as in Fig. 2A. Each bar represents the %GFP$^+$ cells in an individual colony. The last bar on the right represents the %GFP$^+$ cells in the seeding culture. (**A**) A simulation of a strain with 30% GFP + cells in the seeding culture and 9% A → S and 5% S → A conversion rates per generation. (**B**) A simulation of a strain with 60% GFP + cells in the seeding culture and 5% A → S and 3% S → A conversion rates. (**C**–**H**) Conversion rates in the strains indicated on the top of each graph

of lower or higher bars at the flanks of the graphs indicates a reduced rate of epigenetic conversions.

In Fig. 5C–H, we present the graphs produced by our single and double deletion mutants. Based on the simulation in Fig. 5A, in the *BY4742* strain, the conversion rates of the *HTB1-yEGFP* construct are approximately 9% A → S and 5% S → A per generation (Fig. 5C). The plot produced by the *cac1*Δ strain is consistent with a decrease in the S → A conversions at this locus (Fig. 5D). For example, out of 36 mini-cultures, three showed less than 10% yEGFP$^+$ cells, while the proportion of GFP$^+$ cells in the seeding culture was 63%. A reduction in the A → S conversions can also

explain the abundance of mini-cultures with high proportion of GFP$^+$ cells (Fig. 5D). The plot produced by the *asf1*Δ strain was similar to the plot produced by *BY4742* with some indication of reduced A → S conversions (Fig. 5E). The plot produced by the *tof1*Δ strain indicated a reduction in the overall frequency of conversion rates, but less pronounced as compared to the *cac1*Δ strain (Fig. 5F). In the *tof1*Δ*cac1*Δ strain, the distribution of yEGFP$^+$ cells in the plot indicated conversion rates higher than in the *BY4742* strain but lower than the *cac1*Δ strain (Fig. 5G). Hence, these observations support the idea that the reduction of conversion rates in *cac1*Δ is reversed by the deletion of *TOF1*. Similar effect was observed at the *HMLα*, but not the *FLO11* locus. Interestingly, the deletion of *TOF1* in the *asf1*Δ background produced a plot similar to the one observed in the *cac1*Δ strain while neither *tof1*Δ nor *asf1*Δ strains displayed a similarly strong phenotype (Fig. 5H). This outcome is consistent with the notion that the deletion of *TOF1* can exacerbate the silencing deficiency of *asf1*Δ and that these effects can also be linked to the conversion rates at this locus.

Discussion

The mechanisms of silencing at the mating type, the sub-telomeric, the *FLO* genes, and the *rRNA*-array loci are well understood (Gartenberg and Smith 2016; Shaban et al. 2021), but little is known on how the passage of replication forks affect the epigenetic state and epigenetic conversions in them (Rowlands et al. 2017; Stewart-Morgan et al. 2020). In this study, we addressed this question by combinations of deletions in genes that encode histone chaperones engaged in replication-coupled chromatin reassembly (*CAC1* and *ASF1*) and factors that work at paused replication forks (*TOF1* and *RRM3*) (Stewart-Morgan et al. 2020). *CAC1* encodes a subunit of CAF-1, which travels behind the fork through an association with the replication clamp PCNA (*POL30*), while Asf1p is believed to travel ahead of the fork. *TOF1* encodes a component of the FPC, while *RRM3* encodes a DNA helicase believed to rescue stalled forks (Shyian and Shore 2021). Recent structural studies indicate that Tof1p/Csm3p associate with the fork ahead of the MCM helicase (Baretić et al. 2020). Because Rrm3p interacts with PCNA, it is believed that it travels behind the fork (Schmidt et al. 2002).

TOF1 and RRM3 regulate gene silencing in conjunction with CAF-1 and ASF1

In this study, we found that the deletion of *TOF1* reduced the loss of silencing in *cac1*Δ cells but enhanced the loss of silencing in *asf1*Δ cells at both the *VIIL* telomere and *HMLα* (Figs. 2 and 4). The deletion of *RRM3* in both *cac1*Δ and *asf1*Δ cells reduced silencing. Hence, we demonstrate that *TOF1* (and potentially the FPC) and *RRM3* are involved in gene silencing and that their functions are connected to the functions of the replication-coupled chaperones CAF-1 and ASF1. We have not observed similar loss of silencing in cells harboring a deletion of *PIF1*. *PIF1* encodes a DNA helicase homologous to *RRM3* and is known to promote DNA replication through G-quadruplex motifs on DNA (Pohl and Zakian 2019; Paeschke et al. 2011). On the other hand, *RRM3* is necessary for rescuing paused replication forks at positions of tightly bound DNA proteins (Sauty et al. 2021). While it is preliminary to address if G-quadruplexes affect gene silencing, our current results and the known activities of *TOF1* and *RRM3* suggest that the mechanisms behind the observed genetic interactions operate at replication forks paused at positions of tightly bound proteins.

It is established that Tof1p directly interacts with Topoisomerase I (Park and Sternglanz 1999) and that this interaction could be significant in the regulation of fork pausing (Shyian et al. 2020). It has also been shown that amino acids 762–830 of Tof1p are critical for the pausing of the replication forks and for sensitivity to DNA damage (Westhorpe et al. 2020). In Fig. 2E, we have demonstrated that the deletion of this portion of Tof1p leads to substantial loss of silencing at the telomeres but does not completely phenocopy the loss of *TOF1*. These results strongly suggest that the pausing of the fork has a major effect on the silencing of genes at the sub-telomeres. At the same time, the differences in the effects of the deletion *TOF1* and the *tof1-762*Δ truncation indicate a more complex mechanism. For example, it is not clear to what extent these truncations affect the interaction with Top1p. The exploration of the physical interaction between Tof1p and FACT (Safaric et al. 2022) via genetic analyses is also of interest. As for *RRM3*, apart from its physical interaction with PCNA (Schmidt et al. 2002), little is known about its mode of action. In Fig. 6, we present a model that summarizes our findings and the possible mechanism that can lead to the observed effects.

Previous studies have indicated that CAF-1 and ASF1 function in distinct genetic pathways at the mating type loci and the telomeres. For example, loss of gene silencing at the telomeres and *HML* locus is exacerbated by the deletion of the histone chaperone Rtt106 in *cac1*Δ but not *asf1*Δ cells (Sharp et al. 2001; Jeffery et al. 2013; Janke et al. 2018). On the other hand, the deletion of clamp loader ELG1 reduces the silencing at *HML* in *asf1*Δ but not *cac1*Δ cells (Janke et al. 2018). Our findings support the notion of the functional and mechanistic distinction between these two histone chaperones. Specifically, we demonstrate that the deletion of *TOF1* has opposite effects in *cac1*Δ and *asf1*Δ cells. It is possible that these differential effects are linked to the physical proximity of FPC

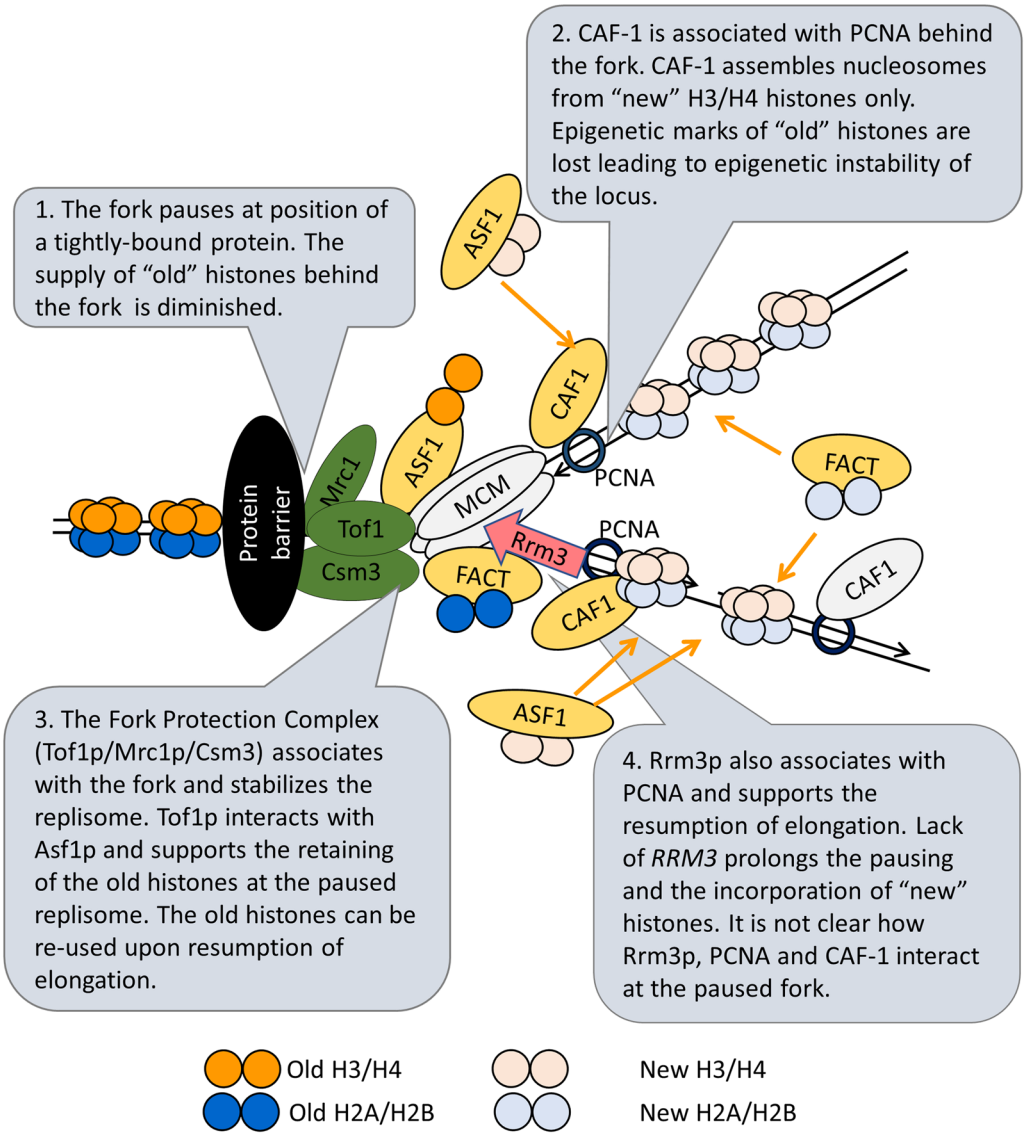

Fig. 6 A model for the interaction between histone chaperones, FPC and Rrm3p at paused replication forks

and ASF1 ahead of the fork and the distortion of the helicase-polymerase conformation upon pausing of the replisome. In addition, the deletions of *RRM3* and *TOF1* have opposite effects on the stability of the paused forks at the *rRNA* gene array (Mohanty et al. 2006; Bastia et al. 2016) but seem to act independently of each other (Shyian et al. 2020). In earlier studies (Wyse et al. 2016; Rowlands et al. 2019b) and here we have shown that the deletion of *RRM3* in both *cac1*Δ and *asf1*Δ backgrounds leads to significant loss of silencing at all loci tested. On the other hand, our assays in the *rrm3*Δ*tof1*Δ strain did not conclusively show opposite gene silencing activities of these two factors. Further studies are needed to elucidate the mechanisms behind the genetic interactions of these genes.

TOF1 is not involved in the silencing of the FLO11 locus

Here, we show that the effects of the deletion of *TOF1* at the *VIIL* telomere and *HMLα* are not recaptured at *FLO11* (Fig. 3). The silencing of *FLO11* is achieved through an *SIR*-independent mechanism while the silencing at telomeres and *HMLα* is SIR-dependent (Rowlands et al. 2017; Sauty et al. 2021). It is possible that Tof1p communicates with SIR proteins to maintain the silent state. Nevertheless, we favor the idea that forks do not pause at the *FLO* loci. Indeed, fork pausing was not detected at these positions in genome-wide studies in *wild-type* and *rrm3*Δ strains (Ivessa et al. 2003; Azvolinsky et al. 2006). However, if this is true, we need to consider that the effect

of the deletion of *RRM3* at the *FLO11* locus (Rowlands et al. 2019b) (Fig. 3) is not caused by its role in the pausing of the fork, but by another, yet uncovered function of this helicase. Support for this idea comes from the fact that Rrm3p is associated with elongating forks and is required for overall fork processivity in vivo (Azvolinsky et al. 2006). It is possible that Mrc1p is also involved in sensing pausing and in the maintenance of gene silencing. However, we could not address this question in our system, because the deletion of *MRC1* was lethal in conjunction with the deletions of *CAC1* and *ASF1*.

The frequencies of epigenetic conversions reflect the silencing phenotypes of *cac1Δtof1Δ* and *asf1Δtof1Δ*

We conducted extensive analyses of the frequencies of S → A and A → S conversions at the *VIIL* locus. In tune with our earlier study (Jeffery et al. 2013), we demonstrate that the loss of silencing in *cac1*Δ cells is linked to the reduction of the frequency of both S → A and A → S conversions (Fig. 5D). These observations agree with the idea that CAF-1 is engaged in the assembly of H3/H4 tetramers from "new" histones only (Ahmad and Henikoff 2018). If this is the case, at paused replication forks the supply of "old" histones could be reduced thus allowing the deposition of "new" histones and loss of epigenetic marks. The removal of CAF-1 would reduce the deposition of new histones and a greater reduction in S → A rates than the A → S rates will lead to the accumulation of GFP + cells in the culture.

Why does the deletion of *TOF1* reverse this effect? A plausible explanation is Tof1p (and FPC), while stabilizing the paused replisome, also prevents spurious deposition or exchange of histones on the new DNA strands. This activity of FPC could include ASF1, but also other histone chaperones. For example, recent studies have indicated that Tof1p physically interacts with FACT (Safaric et al. 2022) and that efficient replisome progression on chromatin templates in vitro requires FACT (Kurat et al. 2017). On the other hand, it has been suggested that Asf1p, apart from its role in the disassembly of nucleosomes, can also retain the "old" histones in the vicinity of paused forks and supply them upon resumption of elongation (reviewed in (Alabert and Groth 2012). FACT could have a similar role in the retention of H2A/H2B histones at the paused replisome. When this function is lost in *asf1*Δ cells, FPC prevents the deposition of new histones thus contributing to the stability of epigenetic transmission. When both *asf1* and *tof1* are lost, the loss of "old" histones is exacerbated, and epigenetic stability diminishes.

DDK, CAF-1, and Tof1p

Another possibility for the epistatic interaction of *CAC1* and *TOF1* is the involvement of a third factor. It is tempting to speculate that this factor is the Dbf4-Dependent Kinase, DDK. The Cac1p subunit of CAF-1 can be phosphorylated by DDK in both human and budding yeast cell extracts (Gerard et al. 2006; Jeffery et al. 2015) and mutations of the DDK target sites on the yeast *CAC1* lead to loss of silencing (Jeffery et al. 2015; Rowlands et al. 2019a). Tof1p is also phosphorylated upon pausing of the fork and its phosphorylation is linked to the stability of paused replisome (Bastia et al. 2016). However, it is not clear if DDK is the kinase responsible for this effect (Bastia et al. 2016). Still, it is possible that the phosphorylation of these two substrates is coordinated at the paused replisome and the loss of one can affect the activity of the other.

Variations in the outcomes of different gene silencing assays

The recently introduced CRASH assay is remarkably sensitive and detects minor transient loss of silencing at *HMLα* that previous *URA3*/5-FOA assays cannot capture (Janke et al. 2018; Brothers and Rine 2019). On the other hand, our *HTB1-yEGFP* reporter assay is less sensitive than the *URA3*/5-FOA assay (Shaban et al., submitted). It seems that the exposure to 5-FOA detects levels of expression of *URA3, which,* like in the CRASH assays, represent transient loss of silencing at the telomere and not necessarily true epigenetic conversions. Still, our drug-free assay reveals the same trends observed with the *URA3*/5-FOA assays, albeit in significantly narrower range. More importantly, the fact that we see the same genetic interactions with the most (CRASH) and the least (*HTB1-yEGFP*) sensitive assays adds credibility to our analyses and conclusions.

Conclusion

Our findings provide strong evidence about the involvement of *TOF1* (and possibly the FPC) and *RRM3* in maintenance of epigenetic state through interactions with the replication-coupled histone chaperones CAF-1 and *ASF1*. Future studies are needed to add detailed evidence for the mechanisms that govern histone turnover at paused replication forks.

Supplementary Information The online version contains supplementary material available at https://doi.org/10.1007/s00294-023-01273-3.

Acknowledgements The authors would like to thank Dr. M. Oki for providing the *HTB1-yEGFP* construct, Dr. H. Murphy for *FLO11-yGFP-KanMX* construct, and Dr. Jasper Rine for the CRASH strains,

Emma Lessard for help in generating the mutant strains with the *HTB1-yEGFP* construct, the Molecular and Cellular Imaging Facility, University of Guelph for the technical support.

Author contributions KS planned and performed experiments, analyzed data, prepared figures and wrote a draft of the manuscript.AD performed experiments, analyzed data and prepared figures.SMS performed experiments and prepared figures.EL performed experiments and analyzed data.AF performed experiments and prepared figures. KY supervised the study and wrote the final version of the manuscript.

Funding Funding for this study is provided by a grant to KY (RGPIN-2015-06727) from NSERC. KS, AD, AF and SMS are supported by bursaries from the College of Biological Science at the University of Guelph.

Declarations

Conflict of interest The authors declare no competing interests.

References

Ahmad K, Henikoff S (2018) No strand left behind. Science 361:1311–1312. https://doi.org/10.1126/science.aav0871

Alabert C, Groth A (2012) Chromatin replication and epigenome maintenance. Nat Rev Mol Cell Biol 13:153–167. https://doi.org/10.1038/nrm3288

Almouzni G, Cedar H (2016) Maintenance of epigenetic information. Cold Spring Harb Perspect Biol. https://doi.org/10.1101/cshperspect.a019372

Azvolinsky A, Dunaway S, Torres JZ et al (2006) The S. cerevisiae Rrm3p DNA helicase moves with the replication fork and affects replication of all yeast chromosomes. Genes Dev 20:3104–3116. https://doi.org/10.1101/gad.1478906

Baretić D, Jenkyn-Bedford M, Aria V et al (2020) Cryo-EM structure of the fork protection complex bound to CMG at a replication fork. Mol Cell 78:926-940.e13. https://doi.org/10.1016/j.molcel.2020.04.012

Bastia D, Srivastava P, Zaman S et al (2016) Phosphorylation of CMG helicase and Tof1 is required for programmed fork arrest. Proc Natl Acad Sci. https://doi.org/10.1073/pnas.1607552113

Beranek DT, Heflich RH, Kodell RL, Morris SM, Casciano DA (1983) Correlation between specific DNA-methylation products and mutation induction at the HGPRT locus in Chinese hamster ovary cells. Mutat Res 110:171–180. https://doi.org/10.1016/0027-5107(83)90026-x

Brothers M, Rine J (2019) Mutations in the PCNA DNA polymerase clamp of saccharomyces cerevisiae reveal complexities of the cell cycle and ploidy on heterochromatin assembly. Genetics 213:449–463. https://doi.org/10.1534/genetics.119.302452

Deegan TD, Baxter J, Ortiz Bazán MÁ et al (2019) Pif1-family helicases support fork convergence during DNA replication termination in eukaryotes. Mol Cell 74:231-244.e9. https://doi.org/10.1016/j.molcel.2019.01.040

Dodson AE, Rine J (2015) Heritable capture of heterochromatin dynamics in Saccharomyces cerevisiae. Elife 4:e05007–e05007. https://doi.org/10.7554/eLife.05007

Gan H, Serra-Cardona A, Hua X et al (2018) The Mcm2-Ctf4-Polα axis facilitates parental histone H3–H4 transfer to lagging strands. Mol Cell 72:140-151.e3. https://doi.org/10.1016/j.molcel.2018.09.001

Gartenberg MR, Smith JS (2016) The Nuts and Bolts of Transcriptionally Silent Chromatin in Saccharomyces cerevisiae. Genetics 203:1563–1599. https://doi.org/10.1534/genetics.112.145243

Gerard A, Koundrioukoff S, Ramillon V et al (2006) The replication kinase Cdc7-Dbf4 promotes the interaction of the p150 subunit of chromatin assembly factor 1 with proliferating cell nuclear antigen. EMBO Rep 7:817–823. https://doi.org/10.1038/sj.embor.7400750

Gottschling DE, Aparicio OM, Billington BL, Zakian VA (1990) Position effect at S. cerevisiae telomeres: reversible repression of Pol II transcription. Cell 63:751–762

Groth A, Corpet A, Cook AJ et al (2007) Regulation of replication fork progression through histone supply and demand. Science 318:1928–1931. https://doi.org/10.1126/science.1148992

Hastie T, Tibshirani R, Friedman J (2009) The elements of statistical learning. Springer Ser Statist. https://doi.org/10.1007/978-0-387-84858-7

Ivessa AS, Lenzmeier BA, Bessler JB et al (2003) The Saccharomyces cerevisiae helicase Rrm3p facilitates replication past nonhistone protein-DNA complexes. Mol Cell 12:1525–1536

Janke R, King GA, Kupiec M, Rine J (2018) Pivotal roles of PCNA loading and unloading in heterochromatin function. Proc Natl Acad Sci U S A 115:E2030–E2039. https://doi.org/10.1073/pnas.1721573115

Jeffery DC, Wyse BA, Rehman MA et al (2013) Analysis of epigenetic stability and conversions in Saccharomyces cerevisiae reveals a novel role of CAF-I in position-effect variegation. Nucleic Acids Res 41:8475–8488. https://doi.org/10.1093/nar/gkt623

Jeffery DC, Kakusho N, You Z et al (2015) CDC28 phosphorylates Cac1p and regulates the association of chromatin assembly factor I with chromatin. Cell Cycle 14:74–85. https://doi.org/10.4161/15384101.2014.973745

Kurat CF, Yeeles JTP, Patel H, Early A, Diffley JFX (2017) Chromatin controls DNA replication origin selection, lagging-strand synthesis, and replication fork rates. Mol Cell 65:117–130. https://doi.org/10.1016/j.molcel.2016.11.016

Makovets S, Herskowitz I, Blackburn EH (2004) Anatomy and dynamics of DNA replication fork movement in yeast telomeric regions. Mol Cell Biol 24:4019–4031

Mano Y, Kobayashi TJ, Nakayama J et al (2013) Single cell visualization of yeast gene expression shows correlation of epigenetic switching between multiple heterochromatic regions through multiple generations. PLoS Biol 11:e1001601–e1001601. https://doi.org/10.1371/journal.pbio.1001601

Mohanty BK, Bairwa NK, Bastia D (2006) The Tof1p-Csm3p protein complex counteracts the Rrm3p helicase to control replication termination of Saccharomyces cerevisiae. Proc Natl Acad Sci USA 103:897–902. https://doi.org/10.1073/pnas.0506540103

Paeschke K, Capra JA, Zakian VA (2011) DNA replication through G-quadruplex motifs is promoted by the Saccharomyces cerevisiae Pif1 DNA helicase. Cell 145:678–691. https://doi.org/10.1016/j.cell.2011.04.015

Park H, Sternglanz R (1999) Identification and characterization of the genes for two topoisomerase I-interacting proteins from Saccharomyces cerevisiae. Yeast 15:35–41. https://doi.org/10.1002/(SICI)1097-0061(19990115)15:1%3c35::AID-YEA340%3e3.0.CO;2-R

Petryk N, Dalby M, Wenger A et al (2018) MCM2 promotes symmetric inheritance of modified histones during DNA replication. Science 361:1389–1392. https://doi.org/10.1126/science.aau0294

Pohl TJ, Zakian VA (2019) Pif1 family DNA helicases: a helpmate to RNase H? DNA Repair 84:102633. https://doi.org/10.1016/j.dnarep.2019.06.004

Rossmann MP, Luo W, Tsaponina O et al (2011) A common telomeric gene silencing assay is affected by nucleotide metabolism. Mol Cell. https://doi.org/10.1016/j.molcel.2011.03.007

Rowlands H, Dhavarasa P, Cheng A, Yankulov K (2017) Forks on the run: can the stalling of DNA replication promote epigenetic

changes? Front Genet 8:86. https://doi.org/10.3389/fgene.2017.00086
Rowlands H, Shaban K, Cheng A et al (2019a) Dysfunctional CAF-I reveals its role in cell cycle progression and differential regulation of gene silencing. Cell Cycle 18:3223–3236. https://doi.org/10.1080/15384101.2019.1673100
Rowlands H, Shaban K, Foster B et al (2019b) Histone chaperones and the Rrm3p helicase regulate flocculation in S. cerevisiae. Epigenet Chromatin 12:56. https://doi.org/10.1186/s13072-019-0303-8
Rusche LN, Kirchmaier AL, Rine J (2003) The establishment, inheritance, and function of silenced chromatin in Saccharomyces cerevisiae. Annu Rev Biochem 72:481–516. https://doi.org/10.1146/annurev.biochem.72.121801.161547
Safaric B, Chacin E, Scherr MJ et al (2022) The fork protection complex recruits FACT to reorganize nucleosomes during replication. Nucleic Acids Res 50:1317–1334. https://doi.org/10.1093/nar/gkac005
Sauty SM, Shaban K, Yankulov K (2021) Gene repression in S. cerevisiae—looking beyond Sir-dependent gene silencing. Curr Genet 67:3–17. https://doi.org/10.1007/s00294-020-01114-7
Schmidt KH, Derry KL, Kolodner RD (2002) Saccharomyces cerevisiae RRM3, a 5′ to 3′ DNA helicase, physically interacts with proliferating cell nuclear antigen. J Biol Chem 277:45331–45337. https://doi.org/10.1074/jbc.M207263200
Scully R, Elango R, Panday A et al (2021) Recombination and restart at blocked replication forks. Curr Opin Genet Dev 71:154–162. https://doi.org/10.1016/j.gde.2021.08.003
Shaban K, Sauty SM, Yankulov K (2021) Variation, variegation and heritable gene repression in S. cerevisiae. Front Genet 12:630506. https://doi.org/10.3389/fgene.2021.630506
Shaban K, Sauty SM, Fisher A et al (2023) Evaluation of drug-free methods for the detection of gene silencing in *Saccharomyces cerevisiae*. Biochem Cell Biol 101:125–130. https://doi.org/10.1139/bcb-2022-0243
Sharp JA, Fouts ET, Krawitz DC, Kaufman PD (2001) Yeast histone deposition protein Asf1p requires Hir proteins and PCNA for heterochromatic silencing. Curr Biol 11:463–473. https://doi.org/10.1016/S0960-9822(01)00140-3
Shyian M, Shore D (2021) Approaching protein barriers: emerging mechanisms of replication pausing in eukaryotes. Front Cell Dev Biol 9:672510. https://doi.org/10.3389/fcell.2021.672510
Shyian M, Albert B, Zupan AM et al (2020) Fork pausing complex engages topoisomerases at the replisome. Genes Dev 34:87–98. https://doi.org/10.1101/gad.331868.119
Stewart-Morgan KR, Petryk N, Groth A (2020) Chromatin replication and epigenetic cell memory. Nat Cell Biol 22:361–371. https://doi.org/10.1038/s41556-020-0487-y
Sutton A, Bucaria J, Osley MA, Sternglanz R (2001) Yeast ASF1 protein is required for cell cycle regulation of histone gene transcription. Genetics 158:587–596. https://doi.org/10.1093/genetics/158.2.587
Takahashi YH, Schulze JM, Jackson J et al (2011) Dot1 and histone H3K79 methylation in natural telomeric and HM silencing. Mol Cell 42:118–126. https://doi.org/10.1016/j.molcel.2011.03.006
Tyler JK, Adams CR, Chen SR et al (1999) The RCAF complex mediates chromatin assembly during DNA replication and repair. Nature 402:555–560. https://doi.org/10.1038/990147
Westhorpe R, Keszthelyi A, Minchell NE et al (2020) Separable functions of Tof1/Timeless in intra-S-checkpoint signalling, replisome stability and DNA topological stress. Nucleic Acids Res 48:12169–12187. https://doi.org/10.1093/nar/gkaa963
Wyse B, Oshidari R, Rowlands H et al (2016) RRM3 regulates epigenetic conversions in Saccharomyces cerevisiae in conjunction with chromatin assembly factor I. Nucleus 7:405–414. https://doi.org/10.1080/19491034.2016.1212796
Yankulov K (2013) Dynamics and stability: epigenetic conversions in position effect variegation. Biochem Cell Biol 91:6–13. https://doi.org/10.1139/bcb-2012-0048
Yeeles JTP, Janska A, Early A, Diffley JFX (2017) How the eukaryotic replisome achieves rapid and efficient DNA replication. Mol Cell 65:105–116. https://doi.org/10.1016/j.molcel.2016.11.017
Yu C, Gan H, Serra-Cardona A et al (2018) A mechanism for preventing asymmetric histone segregation onto replicating DNA strands. Science 361:1386–1389. https://doi.org/10.1126/science.aat8849
Zhang Z, Shibahara K, Stillman B (2000) PCNA connects DNA replication to epigenetic inheritance in yeast. Nature 408:221–225. https://doi.org/10.1038/35041601
Zunder RM, Rine J (2012) Direct interplay among histones, histone chaperones, and a chromatin boundary protein in the control of histone gene expression. Mol Cell Biol 32:4337–4349. https://doi.org/10.1128/MCB.00871-12